Separation Science and Technology
Publication details, including instructions for authors and subscription information:
http://www.informaworld.com/smpp/title~content=t713708471

Differential Geometry Based Continuation Algorithms for Separation Process Applications

W. L. Rion[a]; V. Van Brunt[a]
[a] Department of Chemical Engineering, University of South Carolina, Columbia, S.C.

To cite this Article Rion, W. L. and Van Brunt, V.(1990) 'Differential Geometry Based Continuation Algorithms for Separation Process Applications', Separation Science and Technology, 25: 13, 2073 — 2095
To link to this Article: DOI: 10.1080/01496399008050445
URL: http://dx.doi.org/10.1080/01496399008050445

SEPARATION SCIENCE AND TECHNOLOGY, 25(13-15), pp. 2073-2095 (1990)

DIFFERENTIAL GEOMETRY BASED CONTINUATION ALGORITHMS FOR SEPARATION PROCESS APPLICATIONS

W.L. Rion and V. Van Brunt
Department of Chemical Engineering
University of South Carolina
Columbia, S.C. 29208

ABSTRACT

Nonlinear representation of equilibrium phenomena in azeotropic distillation, extractive distillation and liquid extraction has been shown to result in simulations that have as many as three concentration and temperature profiles that meet the same process specifications. Continuation algorithms are the only assured technique of indicating this multiplicity and solving these highly nonlinear problems. Unfortunately, the robustness of solution is accompanied by increased computation. New procedures that increase the efficiency of these algorithms are documented in this paper.

Local differential geometry is exploited during the continuation procedure to provide a more accurate prediction of the solution trajectory. A rigorous method is documented for accurate prediction of the unit tangent, principal unit normal, and the curvature of the solution path. The resulting computational procedure is significantly more efficient than other continuation methods. It is shown that the effects of increased accuracy of prediction are threefold. The number of a) continuation steps, b)newton corrections to return to the solution path, and c)trajectory prediction failures are all reduced.

When the new algorithm is applied to separation problems involving complex thermodynamic subroutines, evaluation of the system equations represents the major portion of the computation time. Numerical computation of the second order partial derivatives required for the new algorithm requires increased function evaluations. This leads to increased CPU times for large or complex systems. However a quadratic spline approximation to the homotopy path provides an approximation to the differential geometry of the problem that allows the continuation process to proceed without function evaluations during the prediction phase. This results in a significant reduction in function evaluations and computation time required for large or complex separation problems.

Several examples illustrate the new procedure.

INTRODUCTION

In previous research, continuation algorithms have shown multiplicity of concentration profiles for simulation of separation processes. Wayburn and Seader (1) showed that solution multiplicity could be seen in inter-linked systems with ideal liquid solution behavior. Kovach and Seider (2) showed that multiplicity of solution could occur in alcohol dehydration columns. They evaluated the ethanol-water, isopropanol-water, and sec.butyl alcohol-water systems and observed solution multiplicity. In these systems the non-ideal liquid model used, e.g. UNIQUAC, is thought to provide the solution multiplicity. In a second paper, Kovach and Seider (3) showed that simulation results, that could only be obtained by continuation methods, accurately predicted experimental column performance. They noted that the simulation results were extremely dependent on the thermodynamic model used and the values of the interaction parameters.

In this paper a superior continuation method is documented. Based on differential geometry, the new method can reduce the number of prediction steps or function evaluations used to follow the solution trajectory. A comparison with the method of Frantz and Van Brunt (4) is presented. The new algorithm is used to determine the binodal curve for a liquid-liquid

system with difficult solution behavior. A thorough analysis of the solution multiplicity of ethanol dehydration is presented. The theoretical results predict column behavior as a continuous function of energy input to the reboiler.

DIFFERENTIAL GEOMETRY-BASED HOMOTOPY CONTINUATION

The classical Frenet frame analysis used to describe the intrinsic geometry of curves in three-dimensional Euclidean space can be generalized to N-dimensional Euclidean vector space as described in Rion and Van Brunt (5). The continuation procedure presented by Frantz and Van Brunt (4) utilized the local continuation variable technique of Rheinboldt and Burkardt (6) to compute the tangent vector, **T**, of the homotopy path Frenet frame for the predictor of the algorithm. In the differential geometry based procedure the principal unit normal vector, **N**, and the curvature, K, are also computed during the prediction phase of the algorithm. K and **N** are incorporated into the predictor to account for the curvature of the solution path. The curvature also provides a natural means of step-length determination.

Application of the Differential Geometry-Based Procedure to Separation Problems

Calculation of the curvature and principal unit normal for the system $\mathbf{H}(\mathbf{X},t)=0$ (formed by transformation of the original system equations $\mathbf{F}(\mathbf{X})$ by the homotopy $\mathbf{H}(\mathbf{X},t)$) is described in detail in Rion and Van Brunt (5).

Numerical computation of the partial derivatives required in the Rion and Van Brunt algorithm (5) can be costly in terms of CPU time for large or highly complex systems. For these problems a quadratic spline approximation to the solution arc provides an adequate approximation to the differential geometry of the homotopy path without the need of computationally expensive function evaluations. A quadratic spline of the form :

$$x_{i,j+1} = x_{i,j} + a_j(s_{j+1}-s_j) + b_j(s_{j+1}-s_j)^2$$

is formulated around the three most recent points on the homotopy path (which are stored as three, single subscripted, vector arrays.) Each system variable is considered as a continuous homogeneous function of arclength. By requiring continuity of the spline and

linearity of first derivatives, the spline yields the following approximation to the second derivatives with respect to arclength.

$$d^2x_i/ds^2 = 2\xi_{i,2}\{1/d_2(d_1+d_2) + 1/d_2^2\} - 2\xi_{i,1}\{1/d_1(d_1+d_2)\}$$

where

$$\xi_{i,1} = x_{i,j-1} - x_{i,j-2} \; ; \; i=1,\# \text{ system variables}$$
$$\xi_{i,2} = x_{i,j} - x_{i,j-1} \; ; \; i=1,\# \text{ system variables}$$
$$d_1 = s_{j-1}-s_{j-2}$$
$$d_2 = s_j-s_{j-1}$$

The arclength at each step, j, is estimated by:

$$s_j = s_{j-1} + [\sum_{i=1}^{nv}(x_{i,j} - x_{i,j-1})^2]^{1/2} ,$$

where nv equals the number of variables in the homotopy equations.

The curvature is given by:

$$K = [\sum_{i=1}^{nv}(d^2x_i/ds^2)^2]^{1/2} ,$$

and the principal unit normal is found by normalizing $d^2\mathbf{X}/ds^2$;

$$n_i = d^2x_i/ds^2 \; / \; K \; .$$

Numerical experimentation showed that a simple backwards difference approximation to the unit tangent accompanied by a spline based approximation of the principal unit normal and curvature resulted in a more accurate predictor than that using the spline approximation to the unit tangent and principal normal vectors. Thus after the curvature and principal unit normal were calculated as shown above the components of the unit tangent were given simply by:

$$dx_i/ds = (x_{i,j} - x_{i,j-1})/(s_j-s_{j-1})$$

Incorporation of the curvature and principal unit normal into the predictor and step-length procedures is discussed in detail in Rion and Van Brunt (5).

Comparison of Algorithmns for Interlinked CSTR's

The algorithm incorporating the solution curvature into the predictor and step-length was compared to the algorithm of Frantz and Van Brunt on the highly non-linear test problem from Kubicek et al. (7) involving two continuous, non-adiabatic, stirred tank reactors in series, at steady state, with recycle, and an exothermic, first-order, irreversible reaction. The equations describing this system from Kubicek (8) are:

$$f_1=0= (1-R)(1-y_1)\exp\{10\phi_1/(1+10\phi_1/A)\} - y_1$$

$$f_2=0= (1-R)D(1-y_1)\exp\{10\phi_1/(1+10\phi_1/A)\} -10(1+\beta_1)\phi_1 + \beta_1\phi_{c1}$$

$$f_3=0= y_1 - y_2 + (1-R)(1-y_2)\exp\{10\phi_2/(1+10\phi_2/A)\}$$

$$f_4=0= 10\phi_1 - 10(1+\beta_2)\phi_2 + (1-R)D(1-y_2)\exp\{10\phi_2/(1+10\phi_2/A)\} + \beta_2\phi_{c2}$$

The independent variables in these equations are:

y_i = reactant conversion in reactor i= 1 or 2,
ϕ_i = dimensionless temperature in reactor i= 1 or 2,
R = recycle ratio, $R\in(0,1]$.

The physical parameters in the above equations are defined as follows:

A = dimensionless activation energy, $A\in[10,\infty)$,
D = dimensionless adiabatic temperature rise, $D\in[0,60]$,
ϕ_c = dimensionless coolant temperature, $\phi_c\in[-5,2]$,
β_i = dimensionless heat transfer coefficient reactor i,
$\beta_i\in[0,3]$.

In this example, A=1000, D=22, $\phi_{c1}=\phi_{c2}=0$, $\beta_1=\beta_2=2$, $R=0\rightarrow1$.

One desired solution diagram is that of reactor # 2 temperature, ϕ_2, vs recycle rate, R. Solution of this set of equations is very difficult due to strong attraction to a divergent path with negative recycle coordinates.

Figure 1 compares of the progress along the solution path of the Frantz and Van Brunt algorithm and the curvature-based algorithm for this problem. Figure 1 and the accompanying Table 1 show that the curvature-based algorithm required less continuation steps, less Newton corrections, and encountered less correction failures due to poorly chosen step sizes while tracing

the solution path. The number of function evaluations was decreased using analytic derivatives while function evaluations increased when using numerical partial derivatives. CPU time was reduced in both cases, but more when using analytical partial derivatives.

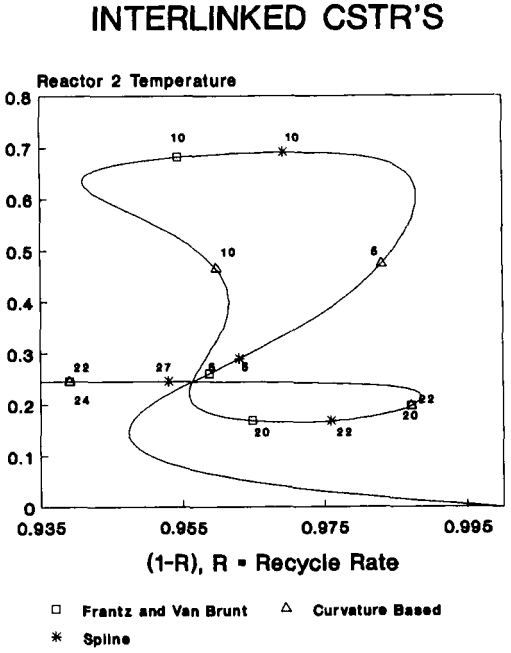

Figure 1. Solution progress comparison for interlinked CSTR's

Table 1. Solution comparison of interlinked CSTR problem.

	Frantz and Van Brunt Algorithm		Curvature Based Algorithm		
Derivatives	Numeric	Analytic	Numeric	Analytic	Spline
# Steps	29	29	24	24	34
# Correctors	60	60	49	49	72
# Failures	19	19	10	10	19
# Functions	718	148	1173	112	667
# Jacobians	114	114	87	87	99
CPU Time (ms)	783	667	740	590	880

Note that the comparisons above were made by relaxing step-length control parameters until algorithm failure occurred and recording the best performance statistics observed. This occurred at the same set of parameters for the Frantz and Van Brunt algorithm and the non-spline based curvature algorithm. The step-length control parameters for the spline based algorithm could not be relaxed to the extent of those of the rigorous algorithm without algorithm failure. Performance of the spline based algorithm at slightly tighter step-length control parameters is shown in Table 1 also. Note that the tighter step-length control results in more steps and corrections taken. The step-length control based on the curvature as determined by the spline is adequate. The spline requires less function evaluations than the Frantz and Van Brunt algorithm using numerical derivatives.

Comparison of Algorithms for Determination of a Liquid-Liquid Phase Envelope

The next example is from Kovach and Seider (2). In this problem the binodal curve for the three component system di-secondary butyl ether (DSBE), secondary butyl alcohol (SBA), and water is the desired homotopy path. The activity coefficients are calculated with UNIQUAC using the interaction parameters of Prausnitz, et al. (9). The binodal curve cannot be generated by use of a standard Newton procedure. The binodal curve can be generated by using a Newton homotopy on the feed composition to an isothermal equilibrium stage. The equilibrium concentrations exiting the stage form the two phase envelope as the feed composition varies between two known pairs of binary equilibrium concentrations. The homotopy equations used are shown below:

$$
\begin{aligned}
H_1 &= (l_1^F)^b\,(1-t) - l_{1_1}^1 - l_1^2 \\
H_2 &= (l_{2_F})^b\,(1-t) - l_{2_1} + t(l_{2_1})^a - l_{2_2}^2 + t(l_{2_2}^2)^a \\
H_3 &= (l_3^F)^b\,(1-t) - l_3^1 + t(l_3^1)^a - l_3^2 + t(l_3^2)^a \\
H_4 &= x_{1_1}\,\gamma_{1_1} - x_{1_2}\,\gamma_{1_2} \\
H_5 &= x_{2_1}\,\gamma_{2_1} - x_{2_2}\,\gamma_{2_2} \\
H_6 &= x_3\,\gamma_3 - x_3\,\gamma_3
\end{aligned}
$$

The path is initiated with the binary streams $(l_i^1)^a$ and $(l_i^2)^a$, which are equilibrium streams from an initial feed stream, $(l^f)^a$, containing only DSBE and water. The path terminates at the feed stream $(l^f)^b$ and its associated equilibrium streams which contain only SBA and water. As the imbedded parameter varies from 1 to 0 the feed stream composition varies continuously between

streams $(l^f)^a$ and $(l^f)^b$. As the feed composition varies, the streams l_i^1 and l_i^2 satisfy the equilibrium constraints H_4-H_6, and determine points on the binodal curve. The resulting binodal curve is shown in Figure 2. The figure also shows the relative progress of the Frantz and Van Brunt algorithm compared to the curvature-based algorithm. A performance comparison of the two algorithms is shown in Table 2.

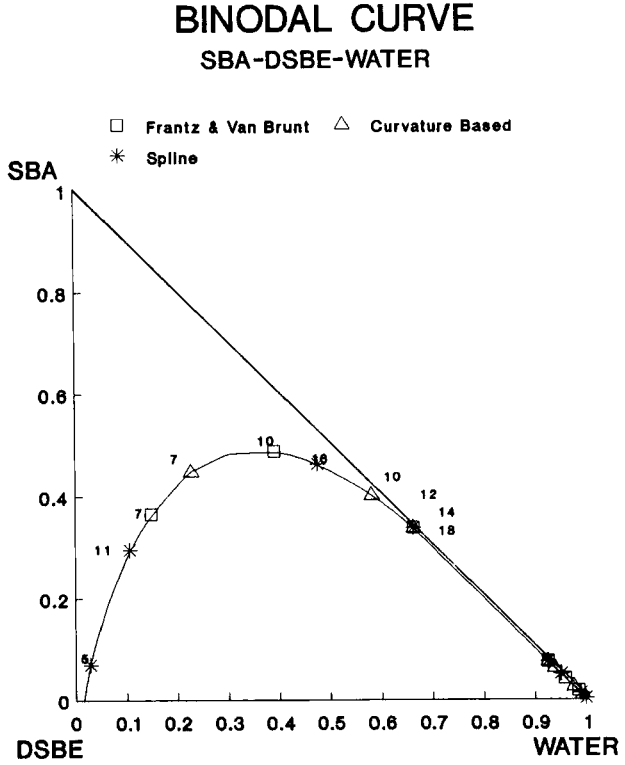

Figure 2. Solution progress comparison for SBA-DSBE-water binodal curve.

Table 2. Solution Comparison for SBA, DSBE, and water binodal curve.

	Frantz and Van Brunt Algorithm	Curvature Based Algorithm	
Derivatives	Numeric	Numeric	Spline
# Steps	14	12	18
# Correctors	41	30	47
# Failures	10	6	5
# Functions	547	1213	471
# Jacobians	67	51	57
CPU Time (ms)	1610	2750	1510

As before the progress of the curvature-based algorithm is greater at each continuation step. Less Newton correctors and step-length failures are encountered. (Only numerical derivatives were used for this system.) Due to the complexity of the system equations the increased function evaluations associated with the curvature-based algorithm lead to increased CPU time. However the spline based algorithm required less function evaluations than the Frantz and Van Brunt algorithm, with less CPU time. As before, more steps and corrections were required for the spline based algorithm due to the required tightening of the step-length control parameters.

ETHANOL DEHYDRATION

An azeotropic system which has received a large amount of interest is the dehydration of ethanol using benzene. The classical azeotropic distillation concentration profiles for this system were first reported by Robinson and Gilliland (10). Magnussen et al. (11) found three different steady states satisfying the same column specifications for this system using UNIQUAC and constant molal overflow in a 27 tray tower. Prokopakis and Seider (12) reported the presence of three different operating regimes with very similar column specifications using the UNIQUAC thermodynamic model with inclusion of the stage energy balances and a

distillate decanter. Their numerical results were obtained using Powell's method (13). Kovach and Seider (2) also investigated this system in a column with a fixed reflux stream and no decanter. Using homotopy continuation they found five steady state solutions with almost exactly the same specifications. Another, more detailed, analysis of this system using Newton-like methods was performed by Venkataraman and Lucia (14). They showed the presence of two turning points in a graph of product purity vs bottoms flowrate. Most recently, Rovaglio and Doherty (15) performed dynamic simulations of this column with a distillate decanter using a UNIQUAC based model that accounted for the possibility of heterogeneous liquid phases. Their work showed the presence of three steady states within a large range of reflux ratio.

Here the above results are extended and amplified using homotopy continuation to further characterize the solution space. The curvature-based algorithm was used to generate the solutions to the MESH equations as a continuous function of reboiler duty by incorporation of the reboiler into a Newton homotopy. Two turning points were observed in the resulting continuation path giving a region where three very different steady state solutions exist for a specified reboiler duty. The solution progress and algorithm efficiencies are compared to that of the Frantz and Van Brunt algorithm.

Simulation Details

Column specifications for the dehydration of ethanol with benzene used in this study are shown in Figure 3. This configuration corresponds to that investigated by Kovach and Seider (2). The non-ideal liquid phase behavior is described by the UNIQUAC equation. The liquid phase is assumed homogeneous. Interaction parameters are the three-component parameter set of Prausnitz et al. (90). The gas phase is assumed to be ideal. The component vapor pressure equations are represented by the extended Antoine equation with the parameters of Gmehling and Onken (16). The component enthalpy equations are those of Reid et al. (17).

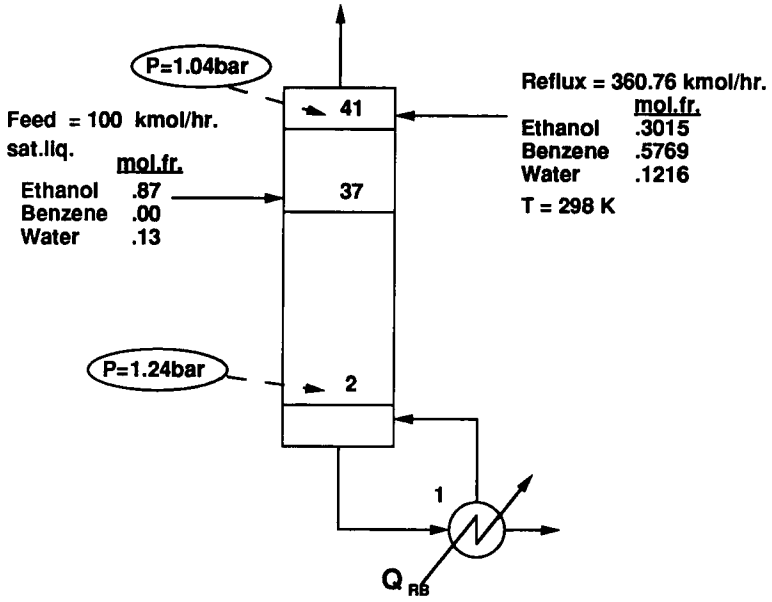

Figure 3. Specifications for the Ethanol Dehydration Tower

The MESH equations for this column were formulated as shown below:

$$l_{i,j+1} + v_{i,j-1} + f_{i,j} - l_{i,j} - v_{i,j} = 0$$

$$l_{i,j+1}h_{i,j+1} + v_{i,j-1}H_{i,j-1} + f_{i,j}h^{f}_{i,j} - l_{i,j}h_{i,j} - v_{i,j}H_{i,j} + Q_j = 0$$

$$P_j\, v_{i,j} / \Sigma v_{i,j} - \gamma_{i,j}\, P^{s}_{i,j}\, l_{i,j} / \Sigma l_{i,j} = 0$$

where,

i = species 1-3,
j = stage number,
$f_{i,j}$ = liquid feed of component i, to stage j,
$h_{i,j}$ = liquid phase enthalpy, component i, stage j,
$H_{i,j}$ = vapor phase enthalpy, component i, stage j,
$h^{f}_{i,j}$ = feed liquid phase enthalpy, component i, stage j,

$l_{i,j}$ = component liquid molar flow rate, species i, stage j,
$v_{i,j}$ = component vapor molar flow rate, species i, stage j,
$P^s_{i,j}$ = component vapor pressure, species i, stage j,
P_j = pressure, stage j,
$\gamma_{i,j}$ = activity coefficient, species i, stage j,
Q_j = energy input to stage j.

The variables associated with each stage were $l_{i,j}$, $v_{i,j}$, and T_j. Q_j was equal to zero for all stages except the reboiler. With the two feed streams and stage pressures in Figure 3 specified, the column has only one degree of freedom unspecified. In this work the reboiler duty, Q_1, was used to fully specify the state of the column.

Homotopy continuation provides a means of rapidly generating the solutions to the MESH equations as a continuous function of reboiler duty. The MESH equations described above were supplemented by a Newton homotopy applied to the reboiler duty for use in the continuation algorithm:

$$Q^i_{RB}\ t + Q^f_{RB}\ (1-t) - Q_1 = 0;$$

where

Q_1 = reboiler duty,
Q^i_{RB} = initial reboiler duty on homotopy path,
Q^f_{RB} = final reboiler duty on homotopy path,
t = imbedded parameter.

As the imbedded parameter t is tracked from 0 to 1 by the continuation algorithm, the reboiler duty varies continuously from Q^i_{RB} to Q^f_{RB}. Thus using these equations the state of the column can be continuously deformed by the reboiler duty. Since the Newton homotopy was applied only to the reboiler specification equation, each point on the solution path represented a physically realistic solution potentially generated by disturbances in reboiler duty.

Simulation Results

The total vapor boilup from the reboiler is shown as a continuous function of reboiler duty in Figure 4. The relative progress of the Frantz and Van Brunt and curvature-based algorithms is shown in Figure 5. A comparison of algorithm performances is shown in Table 3.

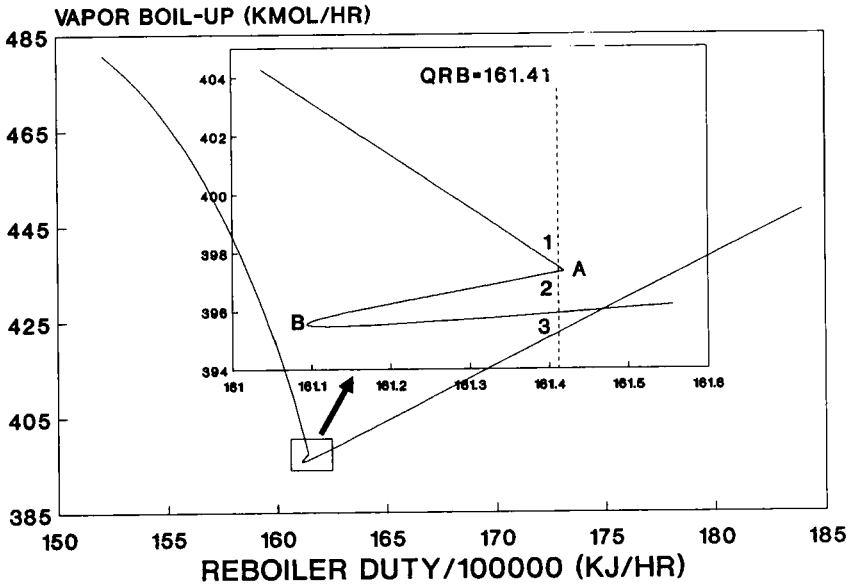

Figure 4. Vapor boil-up vs reboiler duty.

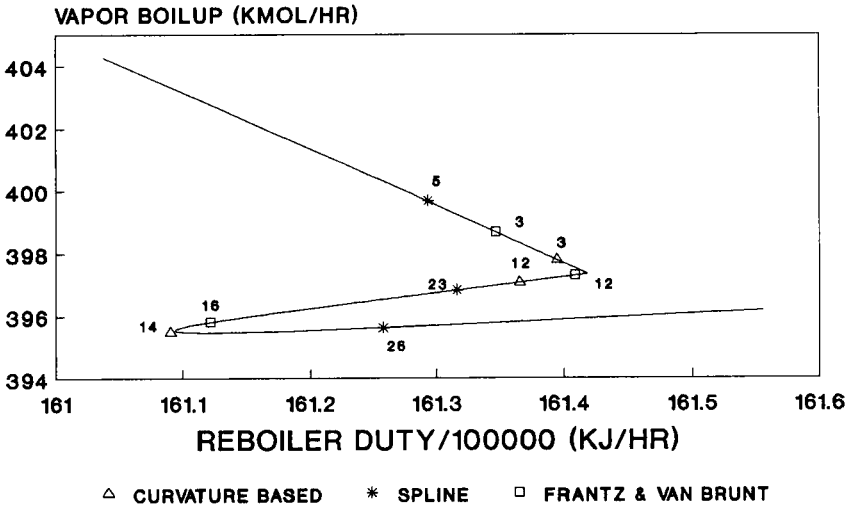

Figure 5. Solution progress comparison for ethanol dehydration tower.

Table 3. Solution Performance Comparison for Ethanol Dehydration Tower.

	Frantz and Van Brunt Algorithm	Curvature Based Algorithm	
Derivatives	Numeric	Numeric	Spline
# Steps	19	16	29
# Correctors	73	63	83
# Failures	0	0	0
# Functions	3409	16382	3160
CPU Time (s)	734	3879	665

The reduction in the number of continuation steps and correctors when using the curvature-based algorithm is consistent with the results on the earlier problems. However, with this complex system, the increased function evaluations associated with rigorous curvature-based algorithm leads to substantially increased CPU time. However the reduction in function evaluations associated with the spline based algorithm results in a reduction of CPU time. Thus the spline based algorithm becomes desirable for large or complex systems of equations associated with separation cascades.

Within a very small range of reboiler duty (161.09-161.42 KJ(10^{-5})/HR) the solution path in Figure 4 goes through two sharp turning points, A and B, yielding a region in which three distinct solutions exist, with three different boilup rates, corresponding to the same energy input to the reboiler. The dotted line in Figure 4 indicates a representative slice through this region. For this slice the three steady state solutions (labeled 1, 2, and 3) corresponding to the same reboiler duty are shown in Figure 6. Figure 6 indicates that for the same reboiler duty the number of trays holding nearly pure ethanol may be a few, more than twenty, or none. At solutions 1 and 2 water is present in appreciable quantities on only the top few stages, benzene is present in significant amounts on sixteen or more stages, and pure, or nearly pure, alcohol is produced. In solution 3 water is present in significant amounts on all stages while benzene is confined to the top six stages. The bottoms concentration in solution 3 corresponds to the ethanol water azeotrope.

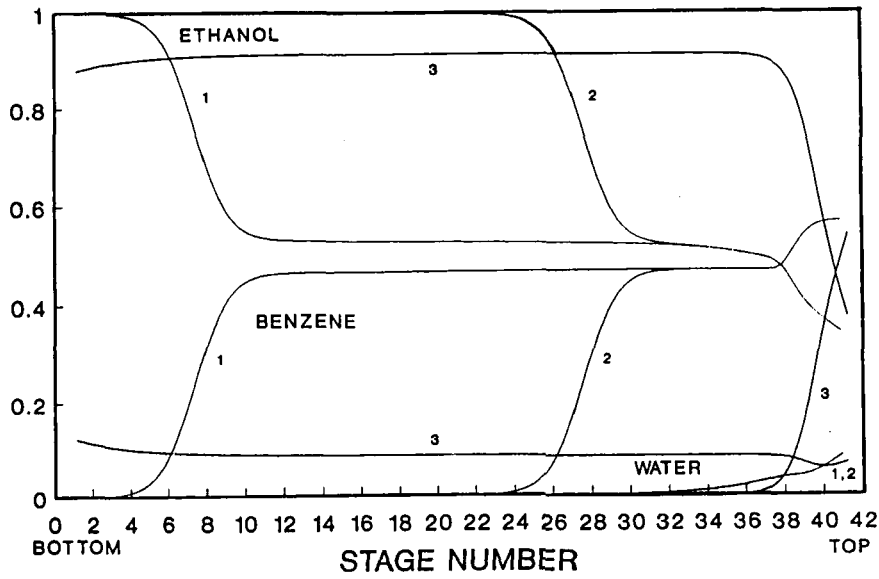

Figure 6. Concentration profiles for QRB=161.41

Column concentration profiles corresponding to turning points A and B are shown in Figure 7. The concentration profiles at turning point A correspond to the classic azeotropic distillation profiles calculated by Robinson and Gilliland (10). The concentration profiles at turning point B correspond to the type III solutions of Kovach and Seider (2). Solutions corresponding to type I, II, IV, and V reported by Kovach and Seider (2) are all within close proximity of solutions 1 and 2.

The solution path of the ethanol concentration in the bottom product stream is shown in Figure 8. Solutions 1, 2, and 3 and turning points A and B are indicated in the figure. The concentration of ethanol increases initially to almost pure ethanol as the reboiler duty is increased, but drops off sharply after turning point A.

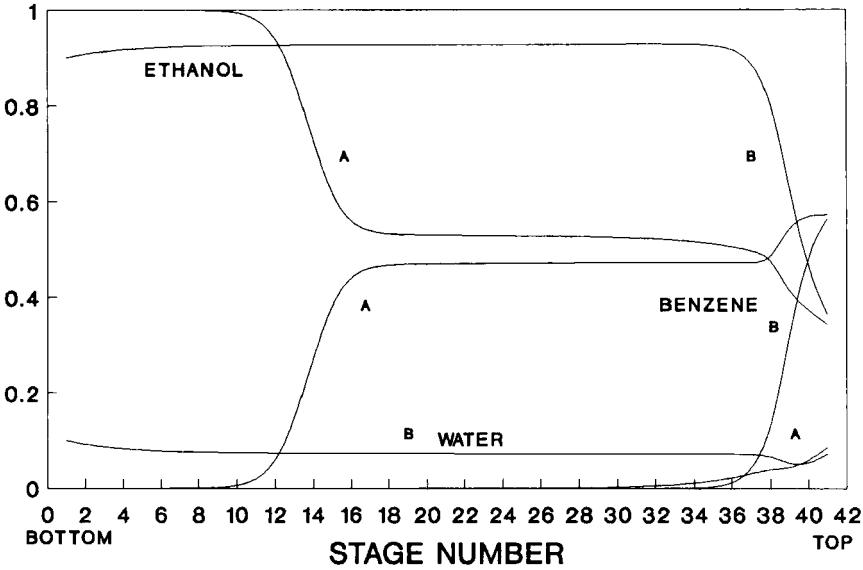

Figure 7. Concentration profiles at turning points A and B.

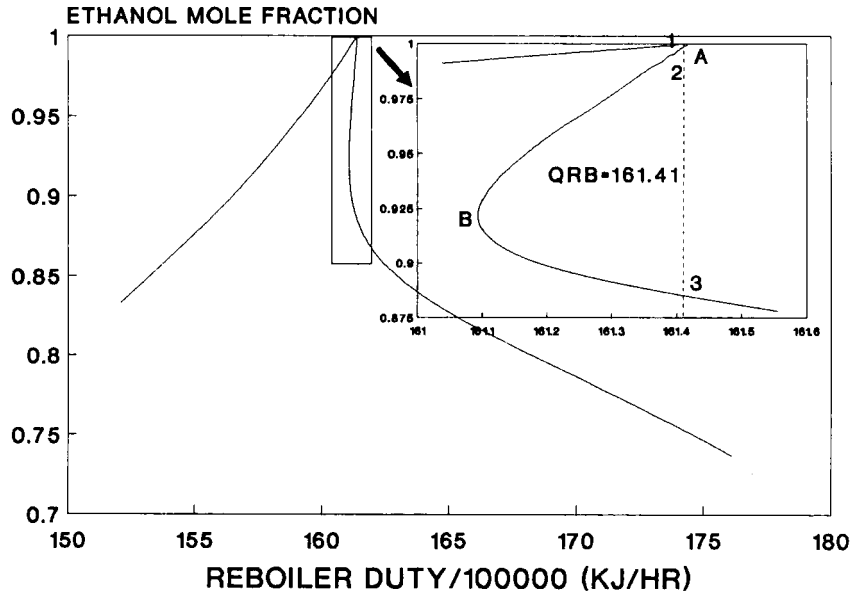

Figure 8. Ethanol concentration in product stream vs reboiler duty.

The corresponding solution path for the column benzene inventory is shown in Figure 9. The benzene inventory decreases sharply at turning point A. Benzene is present in significant quantities on almost every stage for reboiler duties smaller than 161.42 (before turning point A) but is present on only a few stages at any larger reboiler duty. The desired operating conditions are those corresponding to the portion of the path just before turning point A, where a high purity alcohol bottoms product is being produced. Thus Figure 9 shows the importance of maintaining a high benzene inventory (> 15 Kmol benzene/Kmol column liquid) in order to remain at a desirable operating state.

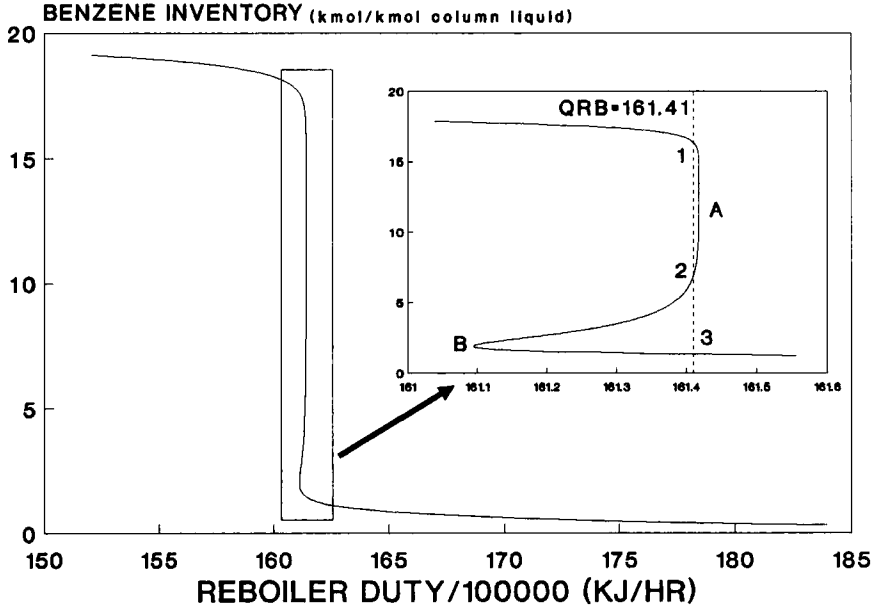

Figure 9. Column benzene inventory vs reboiler duty

The loss of separation associated with a low benzene inventory is explained as follows: Benzene is more volatile than ethanol in the nearly binary mixture in the bottom of the stripping section. Thus as the reboiler duty is increased the number of trays at the bottom of the column holding nearly pure ethanol increases, pushing the benzene concentration front further up the stripping section of the column. However a high benzene concentration must be present in the dehydration zone between the feed stage and the normal concentration fronts in the stripping section to maintain the relative volatility between ethanol and water needed for total dehydration. ($\alpha_{e-w} \approx 0.5$ in the presence of benzene, $\alpha_{e-w} \approx 0.9$ or higher without benzene). Thus as reboiler duty increases through turning point A, the benzene concentration front moves up the column, reducing the number of stages in the dehydration zone, and yielding an insufficient number of stages with adequate benzene concentration for dehydration to occur.

The displacement of the benzene concentration front is accompanied by a displacement of the column temperature front. Figure 10 shows the temperature profiles corresponding to solutions 1,2, and 3, and to turning points A and B. Figure 10 shows that the temperature profile moves up the column as the benzene concentration profile moves up the column. As the temperature profile moves past a given stage in the stripping section, a temperature increase of about 11 °C is realized on the stage. Figure 11 shows how this temperature increase is related to the column benzene inventory. As the temperature on a typical stage (#15) in the stripping section increases from about 345 K to 355 K the column benzene inventory decreases sharply, and thus the desired separation is lost. These findings suggest that perhaps the best way to control the ethanol dehydration column is to monitor the temperature on four or five stages in the stripping section and adjust reboiler duty to maintain the temperature front between stage numbers eight and twenty. As shown in previous figures this would maintain a high benzene inventory and product purity.

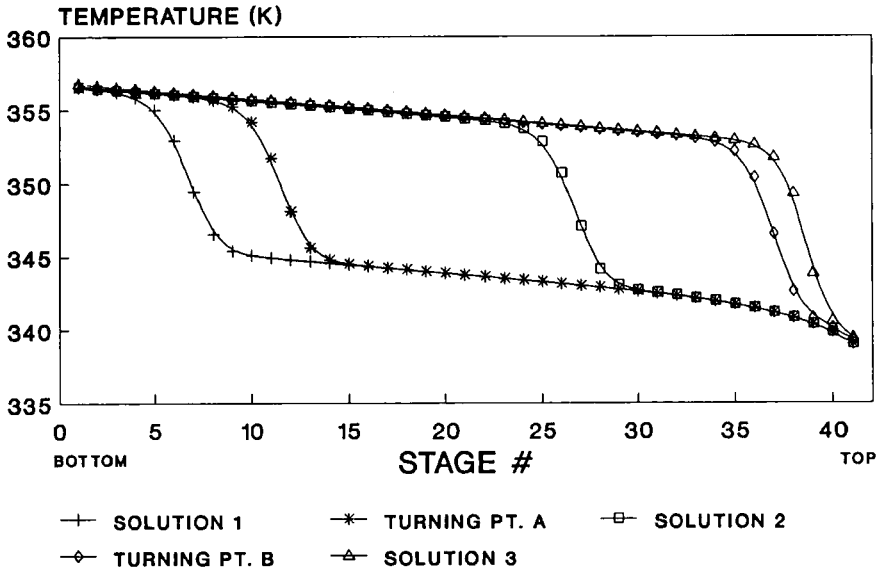

Figure 10. Temperature profiles for ethanol dehydration tower.

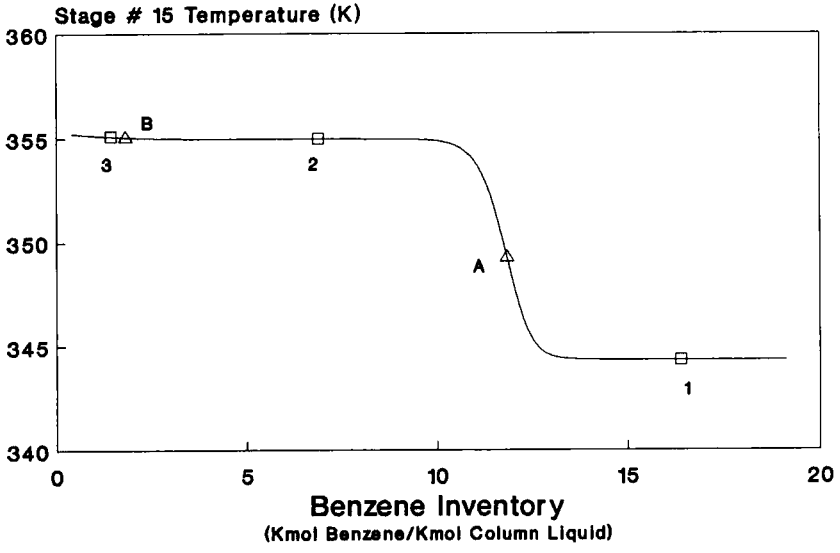

Figure 11. Stage # 15 temperature vs benzene inventory.

CONCLUSIONS

An improved homotopy continuation algorithm has been developed by incorporation of differential geometry into the prediction and step-length phases of the algorithm of Frantz and Van Brunt (4). The new algorithm results in fewer continuation steps and Newton correctors to follow the homotopy path. The curvature-based step-length control is shown to be an improvement. For large or complex systems, such as azeotropic distillation columns, a quadratic spline approximation to the homotopy path provides a reasonable estimate of the differential geometry of the problem, and avoids computationally expensive function evaluations. This results in less function evaluations and reduced CPU time.

The new algorithm can be used to generate the steady states of the dehydration of alcohol with benzene column of Kovach and Seider (2) as a continuous function of reboiler duty. Two turning points are seen in the resulting continuation path giving rise to a region of three steady states corresponding to the exact same column specifications. The importance of a high benzene inventory in the column to maintain the desired product purity is shown. Adjusting reboiler duty to maintain the column temperature front between specified stages provides a means of controlling and maintaining high benzene inventory and product purity.

NOMENCLATURE

A - Dimensionless activation energy.
a_j - Spline fit constant at step j.
b_j - Spline fit constant at step j.
D - Dimensionless adiabatic temperature rise.
d_1 - $s_{j-1}-s_{j-2}$; difference in arclength between steps j-1 & j-2.
d_2 - s_j-s_{j-1}; difference in arclength between steps j-1 & j.
f - Function.
F - Function vector.
$f_{i,j}$ - Liquid feed of component i, to stage j.
$h_{i,j}$ - Liquid phase enthalpy, component i, stage j.
H - Homotopy function vector.
$H_{i,j}$ - Vapor phase enthalpy, component i, stage j.
$h^f_{i,j}$ - Feed liquid phase enthalpy, component i, stage j.
K - Curvature of homotopy path.
$l_{i,j}$ - Component liquid molar flow rate, species i, stage j.
n - Number of problem variables, dimension of F.

N - Unit normal vector of Frenet frame, $\mathbf{N}=\mathbf{C}''(s)/\|\mathbf{C}''(s)\|$.
n_j - Component j of principal unit normal vector.
P_j - Pressure, stage j.
$P^s_{i,j}$ - Component vapor pressure, species i, stage j.
Q_j - Energy input to stage j.
Q_{fRB} - Initial reboiler duty on homotopy path.
Q_{RB}^f - Final reboiler duty on homotopy path.
R - Recycle ratio.
s - Arclength of solution trajectory.
t - Imbedded parameter.
T - Unit tangent vector to homotopy curve.
T_j - Temperature on stage j.
$v_{i,j}$ - Component vapor molar flow rate, species i, stage j.
x - Independent variable.
X - Independent variable vector.
y_i - Reactant conversion in reactor i= 1 or 2.

Greek

α_{e-w} - Relative volatility, ethanol to water.
β_i - Dimensionless heat transfer coefficient reactor i.
$\gamma_{i,j}$ - Activity coefficient, species i, stage j.
$\xi_{i,1}$ - $x_{i,j-1} - x_{i,j-2}$; change in variable i, between steps j-2 & j-1
$\xi_{i,2}$ - $x_{i,j} - x_{i,j-1}$; change in variable i, between steps j-1 & j.
Δs - Step-length used during continuation step.
ϕ_i - Dimensionless temperature in reactor i= 1 or 2.
ϕ_c - Dimensionless coolant temperature.

Superscripts

i - Initial value.
f - Final value.
1,2 - Designation of liquid phase in heterogeneous system.
a,b - Feed stream designation.

Subscripts

i - Component or system variable.
j - Stage subscript, or step number.
n - Signifies nth parameter.
RB - Reboiler.

REFERENCES

1. Wayburn, T.L. and J.D. Seader, "Solutions of Systems of Interlinked Distillation Columns by Differential Homotopy Continuation Methods", Report Chem. Engr. Dept., Univ. Utah (1985).

2. Kovach, J.W. and W.D. Seider, "Heterogenous Azeotropic Distillation - Homotopy Continuation Methods", Submitted to Computers and Chemical Engineering, August, 1986.

3. Kovach, J.W. and W.D. Seider, "Heterogenous Azeotropic Distillation - Experimental and Simulation Results", Submitted to AIChE J., August, 1986.

4. Frantz, R.W. and V. Van Brunt, "A Differential Homotopy Continuation Method for Interlinked Solvent Extraction Cascades", Separation Science and Technology, 22 (2&3), 243-267, (1987).

5. Rion, W.L. and V. Van Brunt, "Differential Geometry Based Homotopy Continuation" , Computers and Chemical Engineering, In press, 1990.

6. Rheinboldt, W.C., and J.V. Burkardt, " A Locally Parameterized Continuation Process." ACM Transactions on Mthematical Software, 9(2), 215-253 (1983).

7. Kubicek, M., H. Hofmann, V. Hlavacek, and J. Sinkule, "Multiplicity and Stability in a Sequence of Two Non-Adiabatic, Non-Isothermal CSTR", Chemical Engineering Science, 35, 987-996, 1980.

8. Kubicek, M., "Algorithm 502, Dependence of Solution of Nonlinear Systems on a Parameter", ACM Trans. Math. Software, 2, 98-107, 1976.

9. Prausnitz, J.M., T.F. Anderson, E.A. Grens, C.A. Ecker, R. Hsieh and J.P. O'Connell, Computer Calcualtions for Multicomponent Vapor-Liquid and Liquid-Liquid Equilibria, Prentice-Hall (1980).

10. Robinson, C.S., and E.R. Gilliland, Elements of Fractional Distillation, Mcgraw-Hill, p.312, (1950).

11. Magnussen, T., M.L. Michelson, and A. Fredenslund, "Azeotropic Distillation Using UNIFAC", Inst. Chem. Eng. Symp. Ser. No. 56, Third Int'l Symp. on Distillation,ICE, Rugby, Warwickshire, England (1979).

12. Prokopakis, G.J. and W.D. Seider, "Feasible Specifications in Azeotropic Distillation", AIChE Journal, (29), 1, (1983).

13. Powell, M.J.D., "A Fast Algorithm for Nonlinearly Constrained Optimization Calculations", presented at 1977 Dundee Conference on Numerical Analysis (1977).

14. Venkataraman, S, and A. Lucia, "Solving Distillation Problems by Newton-Like Methods", Comput. Chem. Eng., 12 (1), 55-69, 1988.

15. Rovaglio, M. and M.F. Doherty, "Dynamics of Heterogeneous Azeotropic Distillation Columns", AIChE Journal, (36), 1, 1990.

16. Gmehling, J., and U. Onken, "Vapor-Liquid Equilibrium Data", DECHEMA, Chemistry Data Series, I, Part 1, Verlag and Druckerei Friedrick Bischoff, Frankfurt, (1977).

17. Reid, R.C., J.M. Prausnitz, and T.K. Sherwood, Properties of Gases and Liquids, Third edition, McGraw-Hill, (1977).